Control System for Regenerative Braking Efficiency in Electric Vehicles with Electro-Actuated Brakes

ARTICLE INFO
Article ID: 10-08-02-0015

doi:10.4271/10-08-02-0015

Control System for Regenerative Braking Efficiency in Electric Vehicles with Electro-Actuated Brakes

Giuseppe Pio Tempone,[1] Henrique de Carvalho Pinheiro,[2] Giovanni Imberti,[2] and Massimiliana Carello[2]

[1]Politecnico di Torino Facoltà di Ingegneria, Dipartimento di Ingegneria Meccanica e Aerospaziale, Italy
[2]Politecnico di Torino, Italy

Abstract

This article presents the design and the analysis of a control logic capable of optimizing vehicle's energy consumption during a braking maneuver. The idea arose with the purpose of enhancing regeneration and health management in electric vehicles with electro-actuated brakes. Regenerative braking improves energy efficiency and allows a considerable reduction in secondary emissions, but its efficiency is strongly dependent on the state of charge (SoC) of the battery. In the analyzed case, a vehicle equipped with four in-wheel motors (one for each wheel), four electro-actuated brakes, and a battery was considered.

The proposed control system can manage and optimize electrical and energy exchanges between the driveline's components according to the working conditions, monitoring parameters such as SoC of the battery, brake temperature, battery temperature, motor temperature, and acts to optimize the total energy consumption. The solution devised allows first to maximize the effects of regenerative braking when the battery SoC is too high to regenerate efficiently, then to safeguard the condition of the battery for both the battery's long life and overheating and safeguard the condition of the brakes to prevent their overheating.

History

Received: 09 Feb 2024
Revised: 25 Mar 2024
Accepted: 11 Apr 2024
e-Available: 01 May 2024

Keywords

Control logic, Braking system, Electric vehicles, Regenerative braking, Electro-actuated brakes, Energy optimization

Citation

Tempone, G., de Carvalho Pinheiro, H., Imberti, G., and Carello, M., "Control System for Regenerative Braking Efficiency in Electric Vehicles with Electro-Actuated Brakes," *SAE Int. J. Veh. Dyn., Stab., and NVH* 8(2):265-284, 2024, doi:10.4271/10-08-02-0015.

ISSN: 2380-2162
e-ISSN: 2380-2170

1. Introduction

One important goal of research in the automotive sector, focused primarily on electric propulsion, is to eliminate combustion emissions from vehicles. The new generation of electric vehicles eliminates local combustion emissions and can regenerate much of the energy by taking advantage of regenerative braking (RB) [1], thus reducing the action of friction brakes, which, in addition to dissipating energy, generate dust emissions due to pad wear.

The new regulations for Euro 7 emissions will consider the "non-exhaust emissions,"—which are particles emitted by tires and brakes of vehicle—as part of the new limitations for passenger vehicles. As shown in the Impact Assessment, it is expected that by 2050 non-exhaust emissions will constitute up to 90% of all particles emitted by road transport [2].

The growing demand for secondary emission reduction will lead to the massive use of RB and, simultaneously, the spread of alternative and electro-actuated braking systems. It will be critical to optimize the control and distribution of braking to maximize its positive effects. In fact, the "traditional car braking system" has always been managed by a hydraulic dual-circuit and it leads to some troubles inherent in the torque split between the axles and wheels since it is not always able to respect the load transfer made during a braking maneuver. So, the problem is that it is not possible with a hydraulic system to integrate a torque divider such that the ideal braking distribution curve is achieved, which ensures that locking does not occur on only one axle.

Liang [3] presents a control logic that maximizes the efficiency of using RB while ensuring stable braking and avoiding unsafe braking conditions. Using an optimization with particle swarms, a nonlinear model is defined for predictive vehicle control in order to modulate the effect of RB.

An important innovation under considerable development in the automotive industry is an innovative car braking system with brake-by-wire (BBW). BBW has an electromechanical brake caliper, allowing the ECU to command each brake independently from electric signals generated by the ECU itself as a function of the torque request. In this way, a better torque split between axles and wheels could be reached, which leads to vehicle dynamics and stability improvement [4]. The automotive industry has invested a great deal in researching control logic inherent in BBW systems. Peng [5] presented a survey on active safety control of X-by-wire electric vehicles: "For active safety control, various control models are summarized, including vehicle dynamics model, single-track model, path tracking model, and wheel dynamics model. Based on the proposed model, different active safety control algorithms are introduced involving longitudinal dynamics control, handling stability control, rollover prevention control, path tracking control, and active fault-tolerant control."

The activation of brakes by electrical signals has enabled the development of braking control logic for electric vehicles that can optimize the energy consumption required by the braking maneuver itself.

As [6] explains, the RB system is not part of the service brake and, due to its heavy battery, the EV brakes are even larger than those of a conventional vehicle. In addition, the close dependence on the regenerative efficiency of the battery SoC leads to the need to size the brakes so that they can independently provide the safety conditions required by regulations. In fact, for example, the RB loses effectiveness at the high SoC [7]. This leads to a reduction in the overall energy efficiency of the vehicle.

Recent researches dealt with the optimization of RB, Shih [8] proposed a control based on the principle of minimum losses to the electric motor in order to achieve the highest value of power regenerative as possible and thus maximize the energy efficiency of the vehicle. Qiu [9] suggested a differentiated control between hydraulically implemented brake and RB, using rotation sensors, where the innovativeness focuses on the use of serial braking logic between regenerative brake and hydraulic brake, which is implemented electrically.

The RB also represents a stress for the battery due to the continuous charge and discharge phase, causing an immediate increase in battery temperature as well as a long-term effect on aging. Feng [10] presented a system designed to preserve battery life by minimizing battery usage during charging phases due to RB, introducing a DC/DC converter with a supercapacitor, with the aim of absorbing the largest peaks of regenerative power.

In this article, the design of a new control logic capable of optimizing the energy consumption and the working conditions of the main components of the driveline (electric motor, electro-actuated brake (BBW), and battery) is presented. Specifically, the logic was applied to an electric vehicle on which four innovative brakes called "magnetorheological" (MR) are implemented. These are a kind of brake of an electro-actuated nature that can generate torque from the change in viscosity of a MR fluid, as a function of a magnetic field passing through it. The proposed control system is developed to complement a direct braking split between the regenerative capacity of the electric motor and the electro-actuated brake with a series of sensors that can consider critical cases for both the brake and the powertrain but also the vehicle dynamics. The innovation of the control logic presented is mainly focused on a working condition, identified as *Disconnected* (explained in detail later), which allows electric power to be regenerated thanks to RB even when the battery is fully charged. This is possible thanks to the presence of electro-actuated brakes (BBW), necessary for the application of the control logic.

2. The Control System

The operating scheme is shown in Figure 1, and it is based on six basic components:

- Battery pack and converter (A, D);
- ECUs (B, C);
- Braking system (E);

FIGURE 1 Operating layout of the control system.

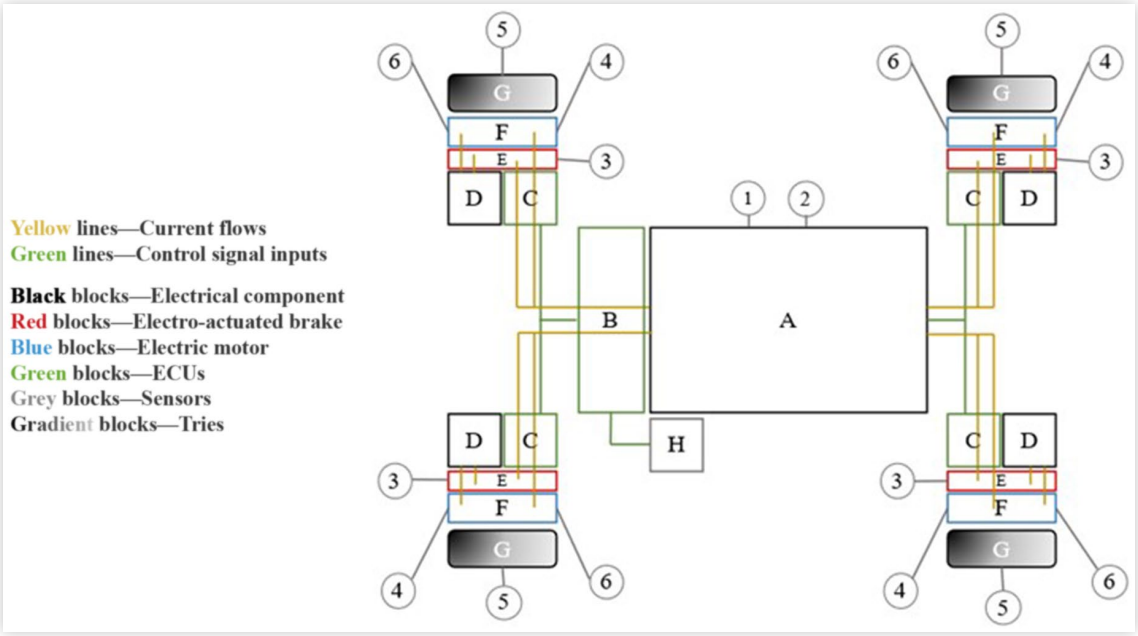

- Electric motor (F);
- Sensors (1–6);
- Input drivers (H).

The control is based on input parameters received from the central ECU, reprocessing the values of vertical force acting on each wheel (due to the presence of a vertical force measurement sensor on the tire, as wheel-mountable commercial load cells) into maximum torque that can be transferred from the tire to the ground and the driver's braking request (H). The values of vertical force, as well as the friction coefficient between tire and road, used in the simulations are the actual values computed by the vehicle model, while in a real application it would be necessary to estimate [11, 12, 13], or to use wheel force transducer (WFT) [14], which is capable of measuring all wheel forces and moments, an essential part of studying and testing vehicle dynamics. The ECU divides the braking demand into four required torque values for each of the vehicle's traction/deceleration systems.

Torque is requested by allocating between RB and electro-actuated braking, following one of the four states (Figure 2):

1. **Baseline**: This braking state involves using the full braking capacity of the RB to recover as much kinetic energy as possible. If RB is not sufficient to have the torque demand from the central ECU on each block (E-F), the same ECU will request the difference between maximum RB and torque demand from the electro-actuated brake, minimizing its use. The battery, in this way, receives a net charge equal to the difference between the regenerated current and the current demanded by the electro-actuated brake.
2. **Disconnected**: In this braking phase, the ECU requests the controller (block D) to isolate the motor and brake actuator (blocks F and E, respectively) from the battery (block A). Braking torque will thus be generated by allocating between the RB and the electro-actuated brake such that the RB will generate enough power to activate the brake to cumulatively achieve the optimum torque to respond to the driver's braking demand. The battery will be neutral to deceleration maneuvers in this configuration, so its SoC will not affect regenerative efficiency.

   In the case considered in this article, electro-actuated brakes are brakes that take advantage of the MR nature of a fluid within them. This fluid changes viscosity as a function of the magnetic field passing through it and generates braking torque. From the characteristics of the MR brake, it is known how much electrical power is required to generate a required braking torque. The logic in *Disconnected* configuration, given a required braking torque for each wheel, calculates how much electrical power needs to be regenerated from the electric motor, then sends a signal to the inverter that drives the motor. This electrical power is sent to the brake, via a DC–DC converter. The amount of power calculated by the logic will then be such that the sum of the braking torques generated by the electric motor and MR brake is equal to the required braking torque.
3. **Full Brake**: The state provides for deactivation of the RB by requesting that the brake (block E) provide the required torque only. The battery in this configuration is in discharge-only mode.

FIGURE 2 Diagram of braking breakdown states per each wheel.

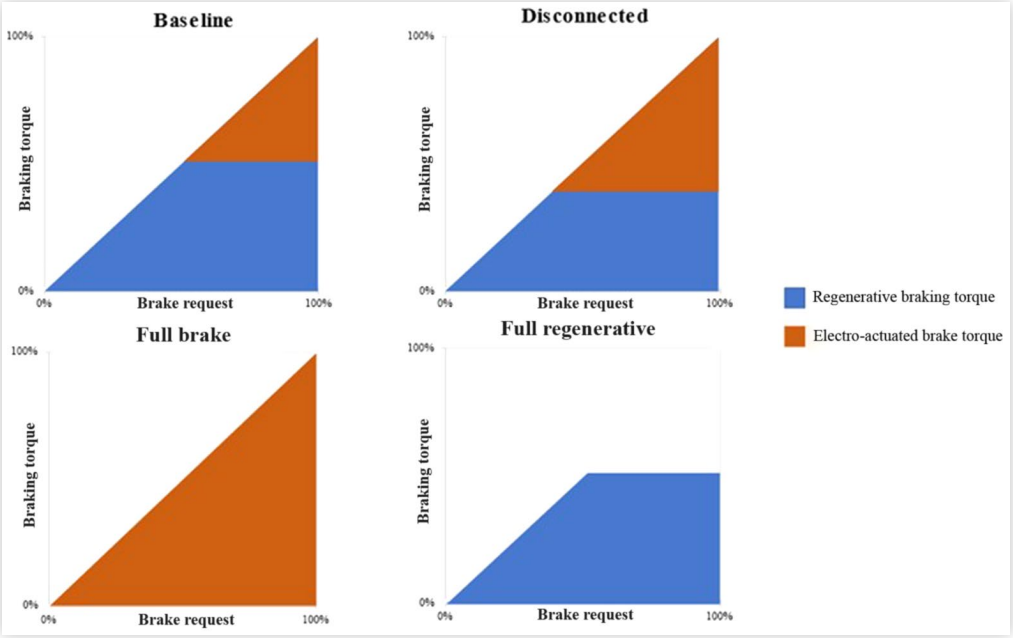

4. **Full Regenerative**: The state provides for brake deactivation (block E) by requesting torque demand exclusively from the RB. This is the only mode (Figure 2) unable to supply 100% of the possible braking demand. For this reason, braking torque would be redistributed to the motors and to the brakes (blocks F and E), but possibly a contribution from the brake is required in case it is the only way to achieve the braking target.

For safety reasons, the brake is equally sized to have 100% braking capacity of the maximum possible required. In this way, the total braking capacity of each block (blocks E and F) is equal to the sum of the capacity of the electro-actuated brake and RB. There cannot be cases where there is insufficient electrical power because logic considers a target value of electrical power required to brake the vehicle from 130 to 0 km/h exclusively with BBW brakes. When the battery reaches this target value (during the discharge phase), the logic gradually slows down the vehicle, signaling an emergency condition for which the battery needs to be recharged.

The central ECU (block B) determines the optimum braking torque for each individual wheel and evaluates the signals received from the peripheral ECUs in order to define the optimum braking state to achieve the target, improving the thermal energy and dynamic conditions of the components.

To achieve the braking target, the ECU prioritizes the baseline state, the stage to which the system will return once each sensor ensures values within the specific standards of each component.

The signals and, consequently, the braking state, follow a specific hierarchical order that goes to define the criticality of the parameters, refer to Figure 1:

1. Battery voltage (sensor 1).
2. Brake temperatures (sensor 3).
3. Battery temperature (sensor 2).
4. Temperature of the electric motor (sensor 4).
5. Rotational speed of the electric motor (sensor 6).

Referring to Figure 3 at each critical condition, the ECU recognizes a different state to be used according to the following criteria:

1. If the SoC exceeds the defined critical value depending on the battery (A), the operating state selected by the central ECU will be in the disconnected mode. This maximizes the RB, which would otherwise be severely limited, and achieves energy optimization for the entire vehicle. Once the SoC decreases below the critical value it will revert to baseline mode.
2. If the brake temperature exceeds a certain value (considered critical for the specific electro-actuated brake system) the central ECU sets the full regenerative state. In this way, the brake is not stressed, and its temperature decreases. Importantly, the full regenerative mode is the only one that is unable to obtain 100% of the potential braking demand from the driver. For this reason, the ECU will have to, if the braking demand exceeds the maximum braking obtainable exclusively with RB, redistribute torques to other electro-actuated brakes that are less thermally stressed, using an activation scheme that keeps the torque generated on the right and left sides homogeneous. If demand is at its maximum, and it is not possible to distribute to the other braking systems, the ECU will prioritize safety

FIGURE 3 Control strategy.

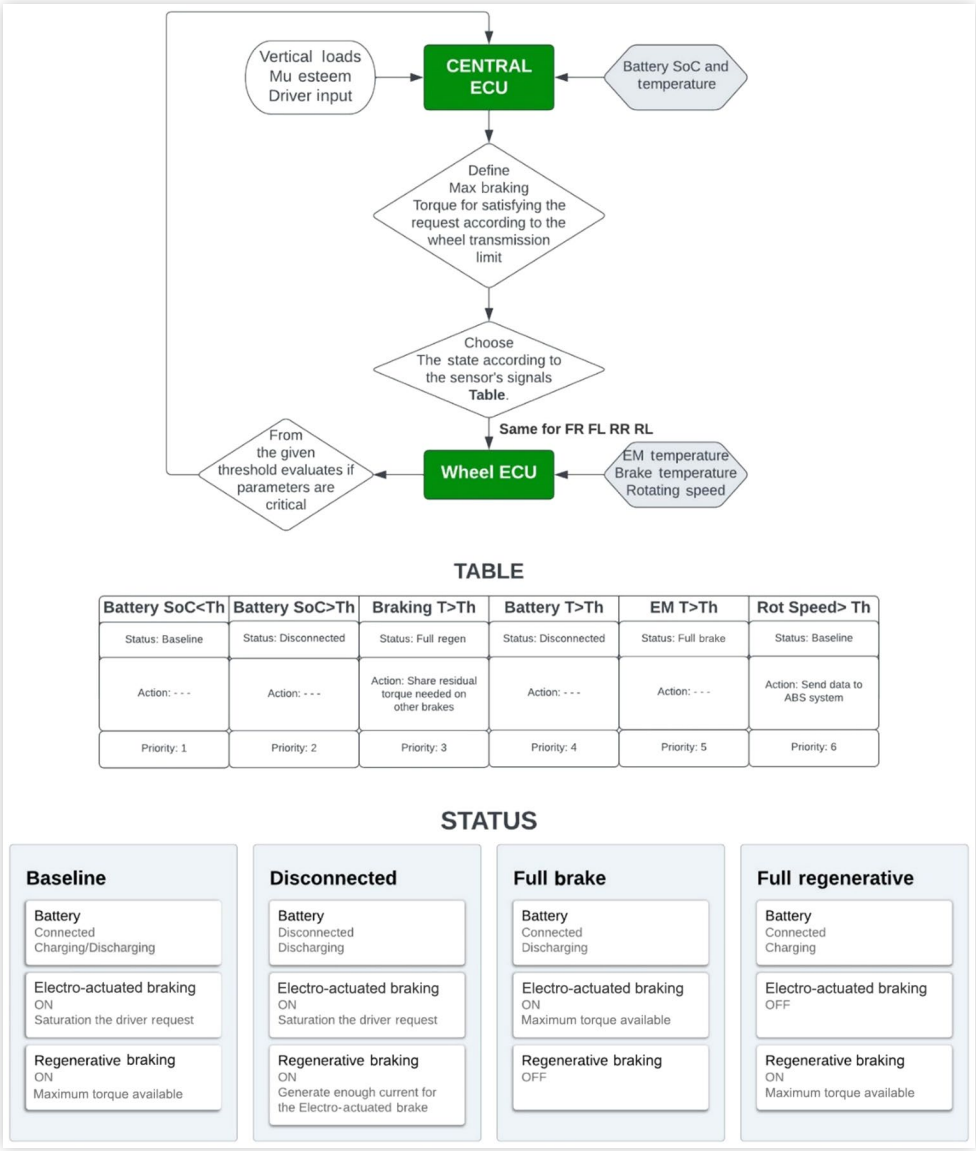

by returning to baseline mode until the vehicle is safe again.

3. If the battery exceeds the critical temperature for the pack, the central ECU sets the disconnected state so that the battery can cool down by reducing charging sessions. Disconnected mode also preserves the battery's life.
4. If the electric motor is overheated, the central ECU sets the full braking state so that the electric motor reduces its temperature. This state is the least energy efficient and is therefore coupled with the least critical condition.
5. If the wheel begins to slip, a dynamically critical condition is registered by the electric motor's rotation sensor in communication with the system's central ECU, which can manage the ABS and ESP control systems, activating them and allowing a stable condition.

3. Transient Braking Control Model

The developed control logic needs to be simulated before moving on to the production and the physical application [8, 9, 15, 16]. So, a properly made from Simulink model has been created to implement data from a specific car, equipped with the innovative electro-actuated braking system, specifically, the car is structured to have the integrated MR brake [17] with an in-wheel motor for each wheel.

The brake, thanks to its special geometry, is integrated with the rotor of the in-wheel motor, thus creating a cavity that can accommodate the MR fluid (MRF). Through a system of coils in the stator of the brake, a magnetic field is generated that passes through the fluid, changing its viscous properties

and thus generating braking torque. An electro-actuated braking system is thus realized that does not exploit the friction between discs and pads and therefore does not generate pollutant emissions [18]. The brake geometry came from the idea of using in-wheel motors as electric motors. The automotive industry has recently been active in research on these kinds of motors because they can lead to advantages in terms of vehicle stability [19], since torque vectoring actuated through individual motor control is more effective than torque vectoring based on active differential [20, 21, 22, 23].

To simplify the explanation, from now on the MR brake and the in-wheel motor mounted on the single wheel will be identified as a zero-emission driving system (ZEDS). It is important to specify that the control logic can be applied and simulated through the model as long as it is a vehicle with at least one electric motor and electro-actuated brakes. So, the only basic requirements for the application of the control logic analyzed are that the vehicle is electric and has an electro-actuated braking system.

The model is able to simulate a road test, supervise the behavior of the vehicle, and monitor parameters such as battery SoC and current, speed and acceleration, drive and RB torque (generated by the MR brakes). The model (in MATLAB/Simulink) has some limitations in validating the developed control logic, in fact, it considers only the longitudinal dynamics, and not the vertical and lateral dynamics. In addition, there is no tire modeling that considers slippage, so the longitudinal force developed by the tires is calculated exclusively through the product of the vertical force transferred to the wheel and the coefficient of friction (assumed to be known and constant). In addition, all thermal signals (motors, brakes, and batteries) are simulated by thermal modeling, which still has an error rate compared with the real case. What is more, in reality, with the algorithm implemented in a vehicle ECU, these thermal signals would come from temperature sensors that would surely exhibit disturbances. The model in its current state does not consider this aspect. However, at present, the main goal is to have initial feedback inherent in the energy effectiveness of the developed logic. Certainly, the next development steps will focus on improving the MATLAB/Simulink model so as to avoid these limitations.

3.1. System Layout

The layout of the model (Figure 4) contains the basic blocks, thanks to which the driving cycle is defined and the test performed, the environmental conditions and data are processed to monitor the behavior of the car, the braking system, the four in-wheel electric motors, and the battery.

As shown in Figure 4, the model is made of several main blocks:

- "**Input Test**": In this block it is possible to select the test you want to perform; in particular, this gives as output the speed profile to be obtained from the vehicle and the slope of the road profile to be traveled by the vehicle in function of its instantaneous position.
- "**Vehicle Dynamics**": The speed profile, the road slope, and the voltage at which the battery is act as the input, and they calculate the torque required for the individual in-wheel motors and the torque required for the MR brakes. In addition, there is a sub-block within the block set to simulate single electric motors, which calculates the torques generated by them and their operating temperatures [24]. Then the relative currents required to these, the total power consumed (during the individual calculation step), and the resulting vehicle dynamics and motion of the vehicle are calculated.
- "**Brakes**": As a function of the required current to the brakes, the braking torque generated by each individual brake and the relative operating temperature of each are calculated [25].

FIGURE 4 Model layout.

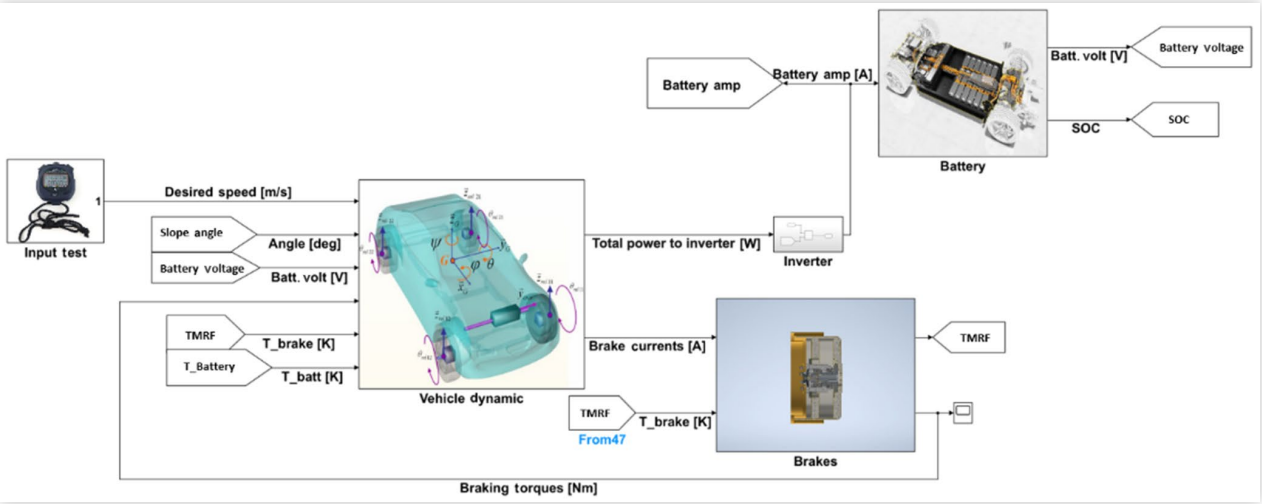

- "**Battery**": Their performance is simulated as a function of the total current required through an inverter that can calculate it according to the total power required by the in-wheel motors and possibly the brakes, then the SoC is provided as output. There is also a sub-block in which the thermal behavior of the battery is simulated, which calculates the battery's operating temperature [26], an important parameter to apply the control logic.

3.2. Implementation of the Control Logic in Simulink Model

The implementation of the control logic on Simulink was realized with the use of two MATLAB functions. The first one has a "Truth Table Subsystem" in which there is a truth table that can identify the braking configuration (baseline, disconnected, full braking, and full regenerative) to be implemented at the ZEDS under consideration. In the second one, according to the established configuration, the required braking torque is allocated between the electro-actuated brake and the electric motor. Depending on the defined configuration and instantaneous working conditions (required torque, motor speed, etc.), the current to be sent to the brake (through a DC–DC converter) of the ZEDS under consideration and the torque generated by the corresponding electric motor are derived.

Opted for the use of a truth table since this way allows us to respect the correct priority given to influential quantities, as the logic described in the Paragraph 2 (reported in the table represented in Figure 3).

3.3. Data Comparison in Different Working Conditions

Several test conditions were simulated using the same electric vehicle setup; specifically, the vehicle is equipped with four ZEDS, one for each wheel, in which four "EMRAX 348 Medium Voltage" [27] in-wheel motors and a battery pack with lithium cells are mounted. The values determining the electric motor parameters and the vehicle dynamics are reported, respectively, in Tables 1 and 2.

Several studies [28] testify to the need to oversize brake discs so that they can dissipate more thermal power and prevent them from ceasing to function properly under a stressful working condition such as the Grossglockner descent. Brake heating, therefore, arises as a major design issue. Choosing to simulate the Grossglockner test presents the possibility of opening up the evaluation of different aspects related to the potential of the brake system. In fact, this test proves to be very valuable for the evaluation of brake heating.

The first test done is the "Grossglockner test," which is a typical test performed to measure the working and stress conditions of a vehicle's brake system. Grossglockner is an alpine road in Austria and presents automotive manufacturers with the opportunity to test under extreme driving conditions. The slope of the road and the desired speed profile have been given in input, respectively, both as a function of vehicle displacement.

TABLE 1 Electric motor parameters.

Electric motor parameters	Values
Peak motor power at max load RPM [kW]	200
Continuous motor power [kW]	91
Maximal rotation speed [rpm]	4500
Maximal motor current [Arms]	400
Continuous motor current [Arms]	190
Maximal motor torque [Nm]	500
Continuous motor torque [Nm]	213
Torque/motor current [Nm/Aph rms]	1.3
Motor efficiency [%]	92–98

However, the increasingly impressive advent of electric motors partly succeeds in reducing the problem. In fact, electric vehicles can take advantage of RB, which not only for energy recovery and reduction in brake pad consumption, but also largely averts the possibility of the brakes being overheated, thus impairing their operation. Due to battery mass, the EV brakes are larger than those of a conventional vehicle; moreover, the regenerative capacity of electric vehicles is highly dependent on the SoC.

Wagner [6] analyzed the potential of downsizing the friction brake by using auxiliary power consumers like the high-voltage heater (HVH), the air-conditioning system (AC) and low-voltage auxiliaries, taking into account their dynamic behavior. a model predictive control (MPC) strategy was used to distribute the power in an optimal way in consideration of the system dynamics, and the result is that the required braking power during the Grossglockner test can be almost completely covered by RB. However, the study is also based on a prediction of auxiliary consumption related to desired comfort in the passenger compartment, which could change from case to case.

To have a more complete demonstration of the validity of the developed control logic, in addition to the four

TABLE 2 Vehicle parameters.

Vehicle parameters	Values
Vehicle mass (with EMs and battery) [kg]	1767
Pilot mass [kg]	80
Wheel radius [m]	0.291
Distance of the CG from the front axle [m]	0.861
Wheelbase [m]	2.152
CG height [m]	0.5376
Friction coefficient [—]	0.7
Rolling resistance coefficient f_0 [—]	0.0136
Rolling resistance coefficient K [m/s^2]	6.5×10^{-6}
Vehicle frontal section [m^2]	2
Aerodynamic drag coefficient Cx	0.33

FIGURE 5 Comparison between *Parallel* (left) and *Baseline* (right) configuration.

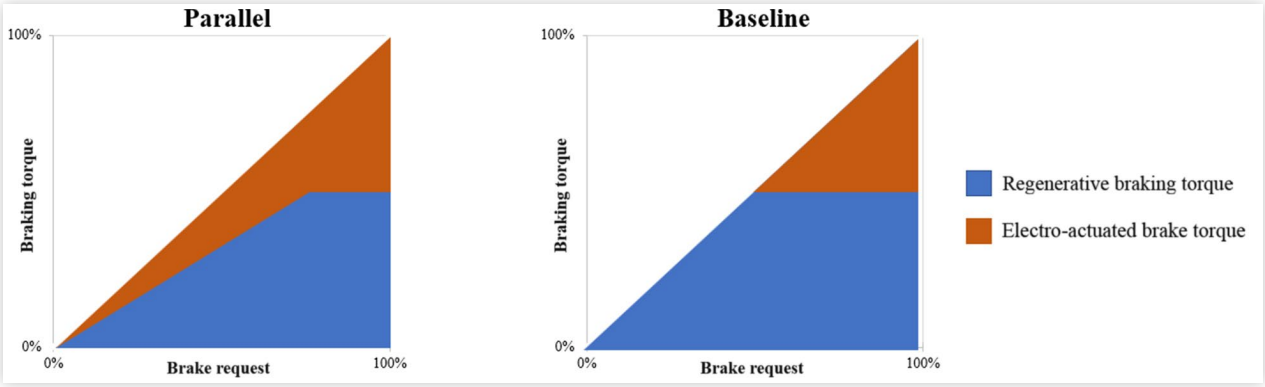

configurations described in Paragraph 2, another configuration called *Parallel* has been considered. It mirrors the operation of the usual control logic acting on electrical machines, whereby given a certain required braking torque, a percentage of torque is supplied by the EM (until the maximum threshold value is reached) and the remainder is supplied by the brake.

A comparison between *Baseline* and *Parallel* configuration is shown in Figure 5.

The *Parallel* configuration was added to allow a comparison of the results obtained with a traditional electric vehicle operated under braking by this configuration and an electric vehicle operated by the developed control logic. In the model considered, the RB contribution according to the required torque was set at 60%. This percentage in commercial electric vehicles does not appear to be constant [29], but it could be set at 60% since the capability of a commercial electric vehicle to regenerate energy usually does not exceed 50%.

4. Simulation Results

The "Grossglockner" test is conducted with an initial battery SoC of 85% and braking configuration in *Parallel*. For convenience, this test is identified as "Test 1." As can be seen in Figure 6, the vehicle is able to follow the desired speed profile sufficiently well, with an average low speed error reaching the peak values just when a remarkable speed variation is requested.

The convention, to obtain a clearer representation, is that the braking torque generated by the MR brake is assumed to have a positive sign, while the RB torque is assumed to have a negative sign. Obviously, to evaluate the vehicle dynamic the braking torques developed by the brakes are considered negative.

The torques generated by the EM and the brake (Figure 7), consistent with the Parallel configuration, the brake always

FIGURE 6 Vehicle and desired speed—Test 1.

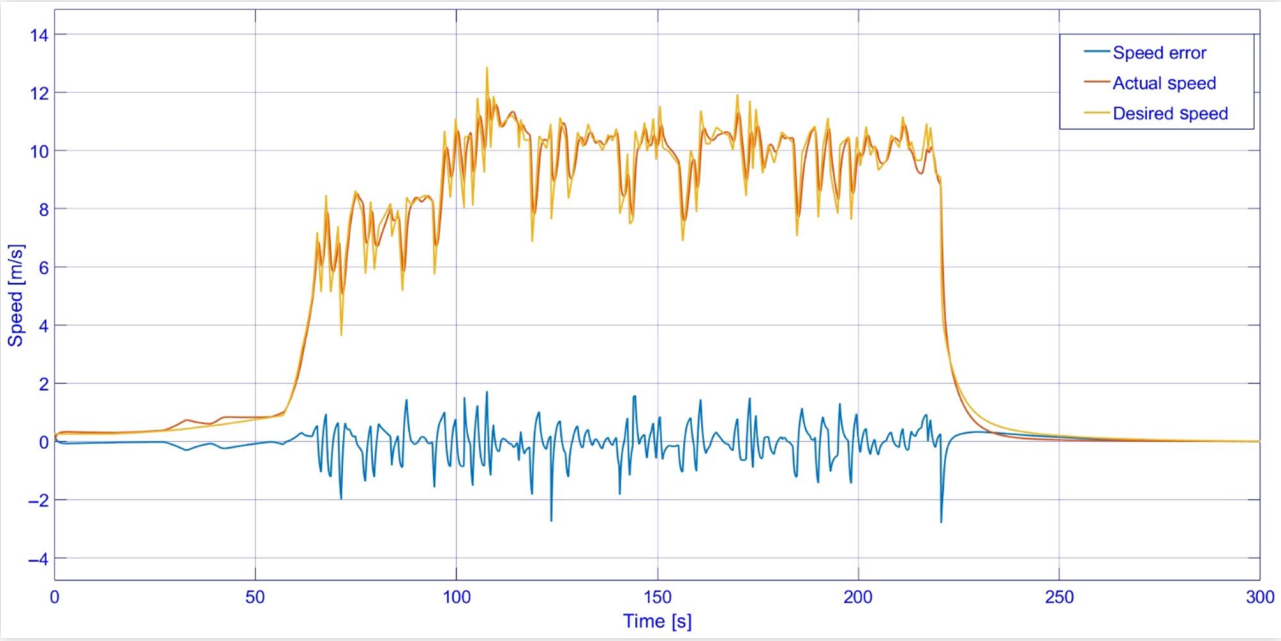

FIGURE 7 Total torque for four motors and four brakes—Test 1.

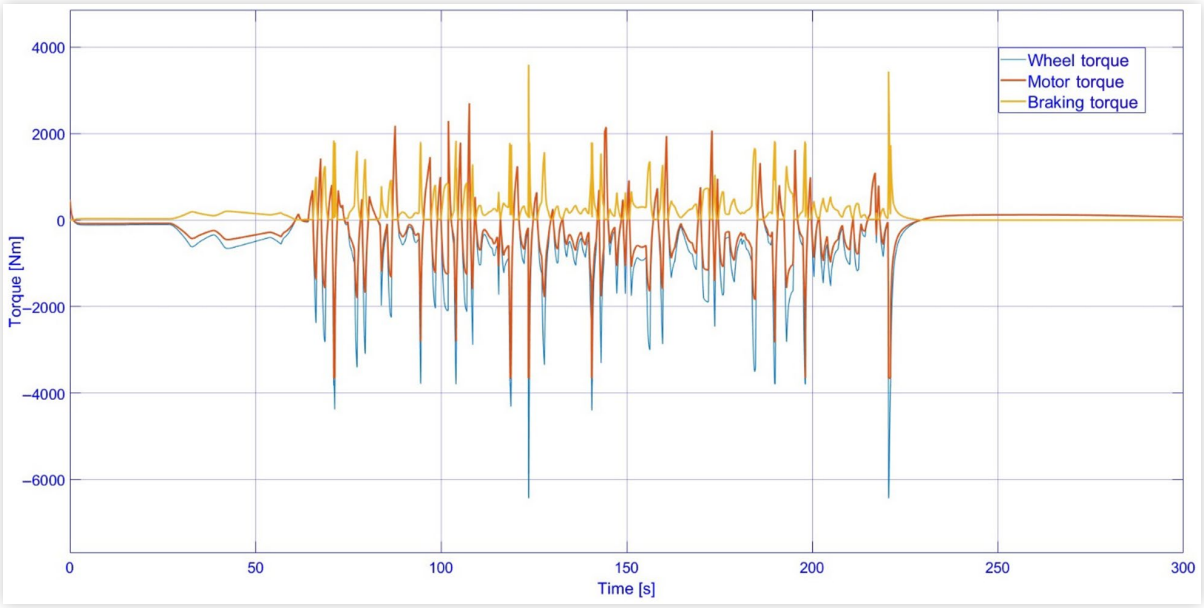

generates braking torque (whenever required) in addition to regenerative torque.

The "Grossglockner" test is simulated again with an initial SoC of 85% but with braking control handled by the control logic explained previously. This test is identified as "Test 2."

The torques generated by the EM and the brake (Figure 8) are consistent with the *Parallel* configuration, the brake always generates braking torque (whenever required) in addition to regenerative torque.

For Test 2, the braking control logic has imposed the *Baseline* configuration; since in most cases the demand for braking torque is never above the maximum threshold guaranteed by the regeneration of the EM, it can be seen in Figure 8 how the MR brake is almost never activated. This is advantageous not only because less frequent activation of the brake keeps the MRF at lower temperatures (Figure 9), but especially from an energy perspective, as the effect of regeneration can be maximized.

Figure 10 shows the SoC that has a higher final value during te Test 2, justifying the energy convenience of the

FIGURE 8 Total torque for four motors and four brakes—Test 2.

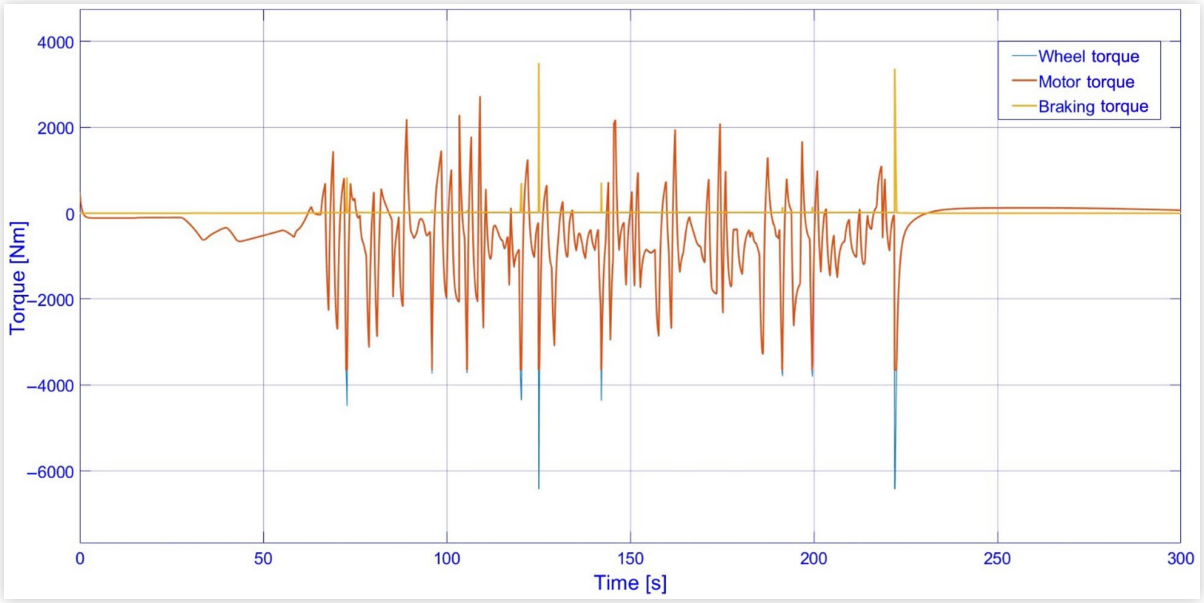

FIGURE 9 MRF temperature [°C] in the left front brake—Test 1 and Test 2.

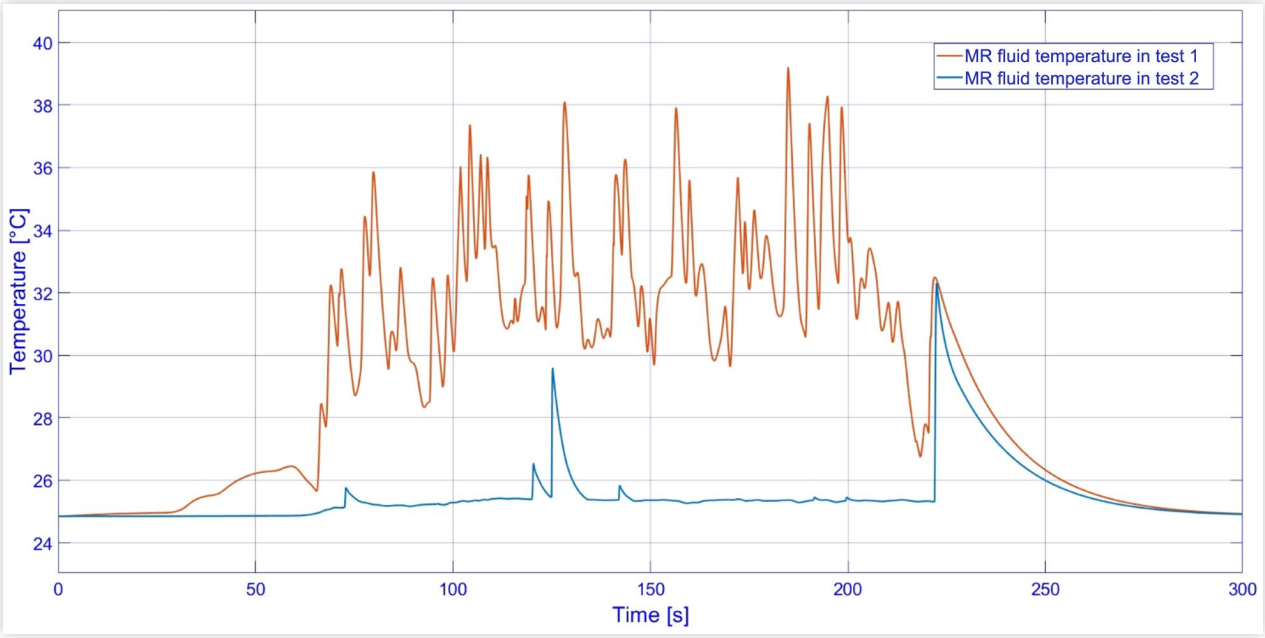

FIGURE 10 SoC—Test 1 and Test 2.

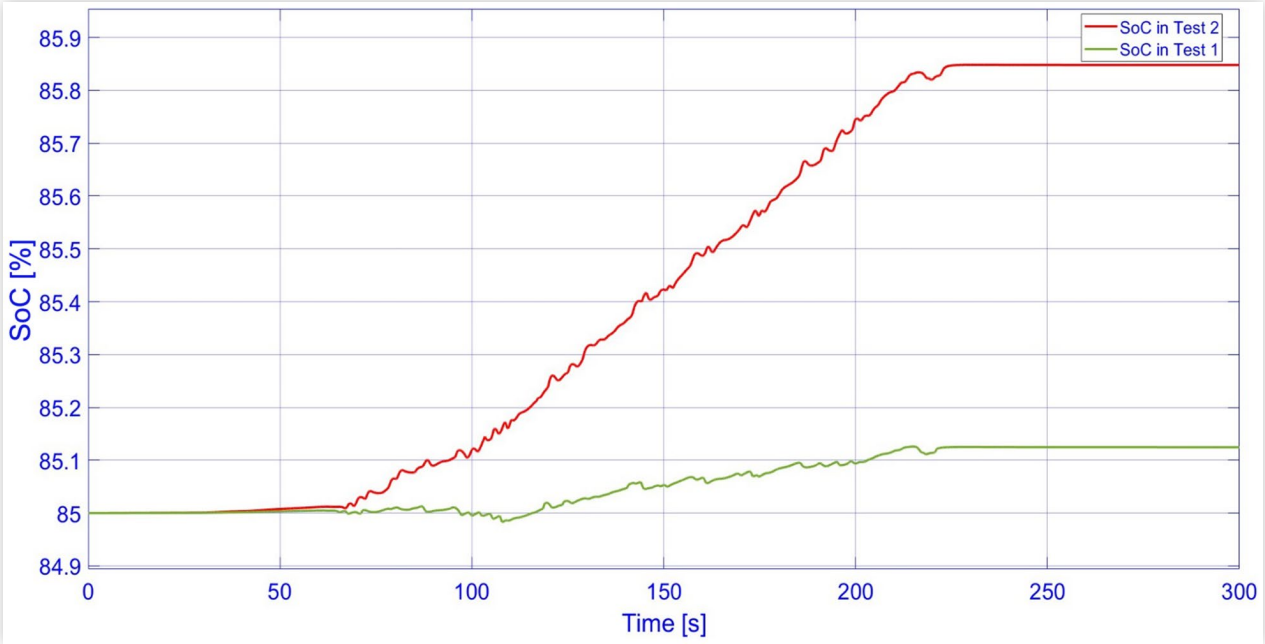

TABLE 3 Results of Test 1 and Test 2.

	Test 1	Test 2	% Difference
Final SoC (%)	85.12	85.85	0.86
Maximum MRF temperature [K]	312.34	302.7	3.09
Energy stored [Wh]	63.52	432.1	580.26

implemented braking control logic proposed by Test 1. The value of stored energy (shown in Table 3) is further evidence of this.

The *Baseline* configuration is more energy efficient than *Parallel*.

However, it is not such as to avert the problem related to the dependence of regenerative efficiency when the SoC exceeds a threshold [7]. So, a "Grossglockner" test is carried out with an initial SoC of 100% in *Parallel* configuration. This value has been chosen just because the RB efficiency decreases greatly when SoC is greater than 98%. This test is identified as "Test 3."

As shown in Figure 11, initially, braking torque is provided solely by the brake since the EM is unable to regenerate torque given the null regenerative efficiency. It is only after 90 s, when the SoC has dropped slightly, that the EM is able to generate negative torque, however, relatively low. Notice that in the *Parallel* configuration, the current given to the MR brake is drawn from the battery.

The "Grossglockner" test has been repeated with an initial SoC of 100% but with braking control handled by the control logic. This test is identified as "Test 4."

The control logic requires a *Disconnected* configuration because the SoC is greater than 98% (Figure 12). In fact, during the braking phase, the EM is always able to provide RB torque, even if only to a small extent.

As shown in Figure 13, the *Parallel* configuration is more energy consuming; in fact, it is possible to note that the behavior of the SoC during Test 3 decreases just when EM gives a positive torque.

The results in Table 4 allow us to conclude that the *Disconnected* configuration built into the control logic is such that it provides significant energy savings even when the SoC is at its maximum. In this way, the regenerative capability of the EM can be released from the SoC and regenerate current even in high states of charge.

A final comparison with "WLTP Brake Cycle" has been made to evaluate the behavior of the main systems of the vehicle over long distances; in particular, this test could be very useful to also evaluate the thermal behavior of the brakes and the behavior of the battery after a long period of working. Initially, a simulation was done with the vehicle without braking control logic, thus in *Parallel* configuration, with an initial SoC of 100%. This test is identified as Test 5.

As can be seen in Figure 14, the "WLTP Braking Cycle" is a much longer test that inevitably puts more stress on major vehicle components such as EM, MR brakes, and battery.

The trend of generated torques is reported in Figure 15.

Initially, there is no regenerative contribution (Figure 16), until the SoC decreases sufficiently to have a regenerative efficiency greater than zero.

Other simulation conditions with "WLTP Brake Cycle" and an initial SoC of 100%, but with the braking control logic active, have been considered. This test is identified as "Test 6."

The trend of generated torques is reported in Figure 17. It's possible to see how the control logic imposes the

FIGURE 11 Total torque for four motors and four brakes—Test 3.

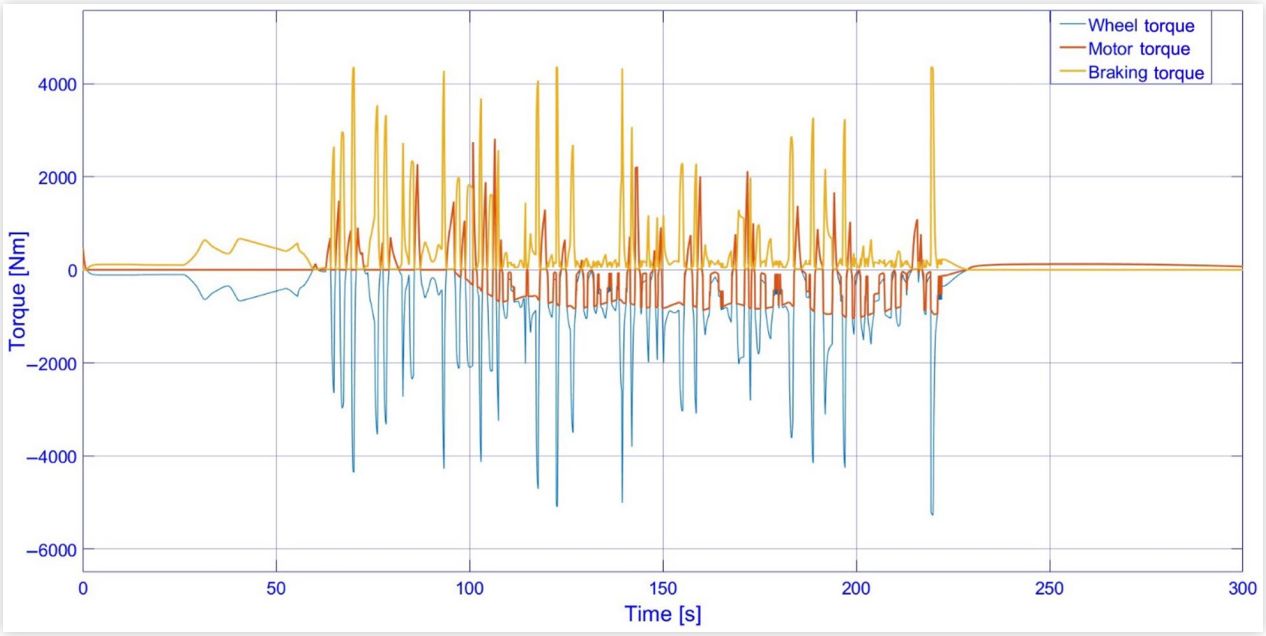

FIGURE 12 Total torque for four motors and four brakes—Test 4.

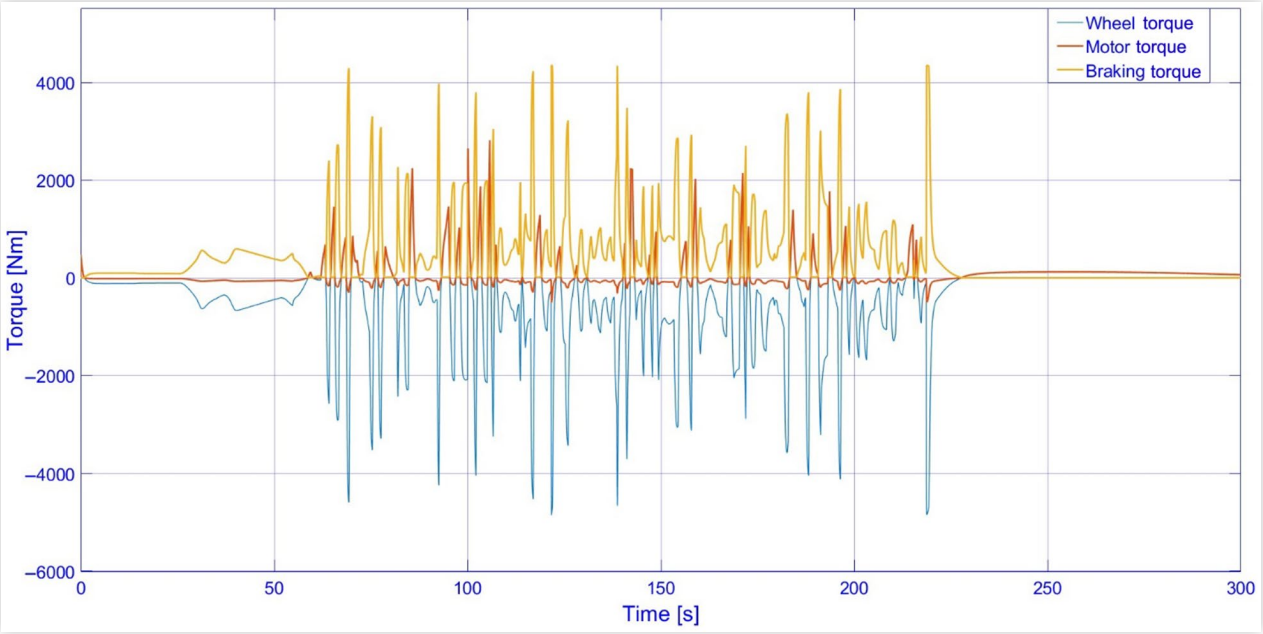

FIGURE 13 SoC—Test 3 and Test 4.

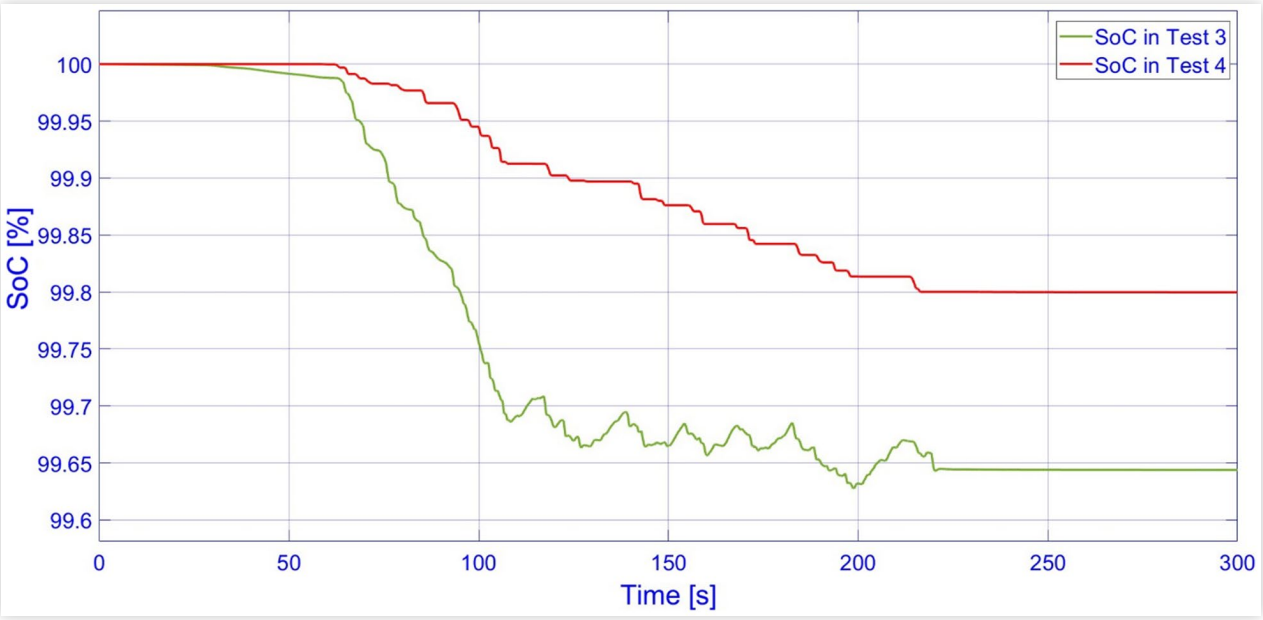

TABLE 4 Results of Test 3 and Test 4.

	Test 3	Test 4	% Difference
Final SoC (%)	99.64	99.8	0.16
Maximum MRF temperature [K]	327.3	333.9	2
Energy stored [Wh]	−187.2	−105.5	43.64

FIGURE 14 Vehicle speed and desired speed—Test 5.

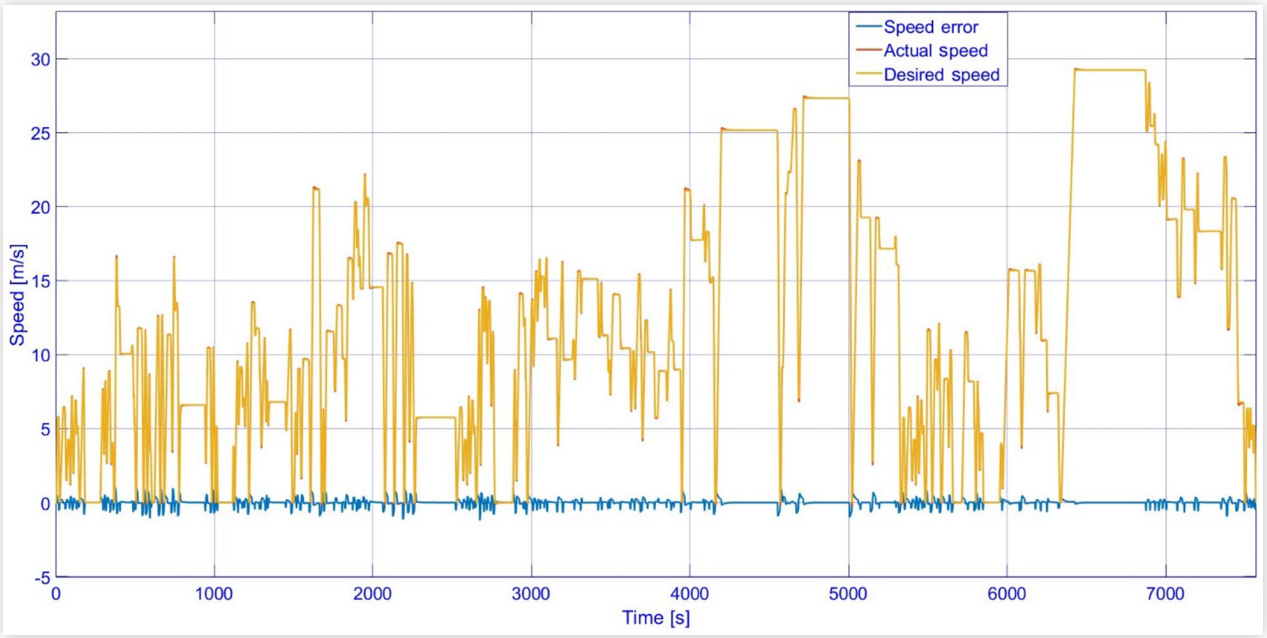

FIGURE 15 Total torque for four motors and four brakes—Test 5.

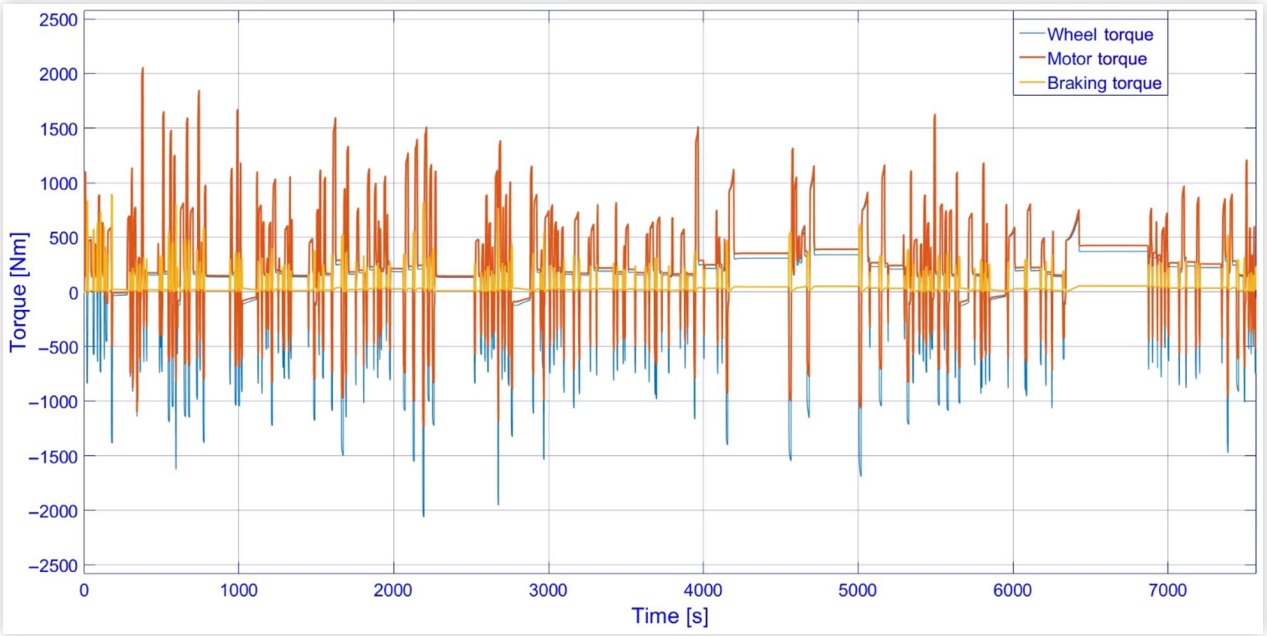

FIGURE 16 Total torque for four motors and four brakes—Test 5 and first 1000 s.

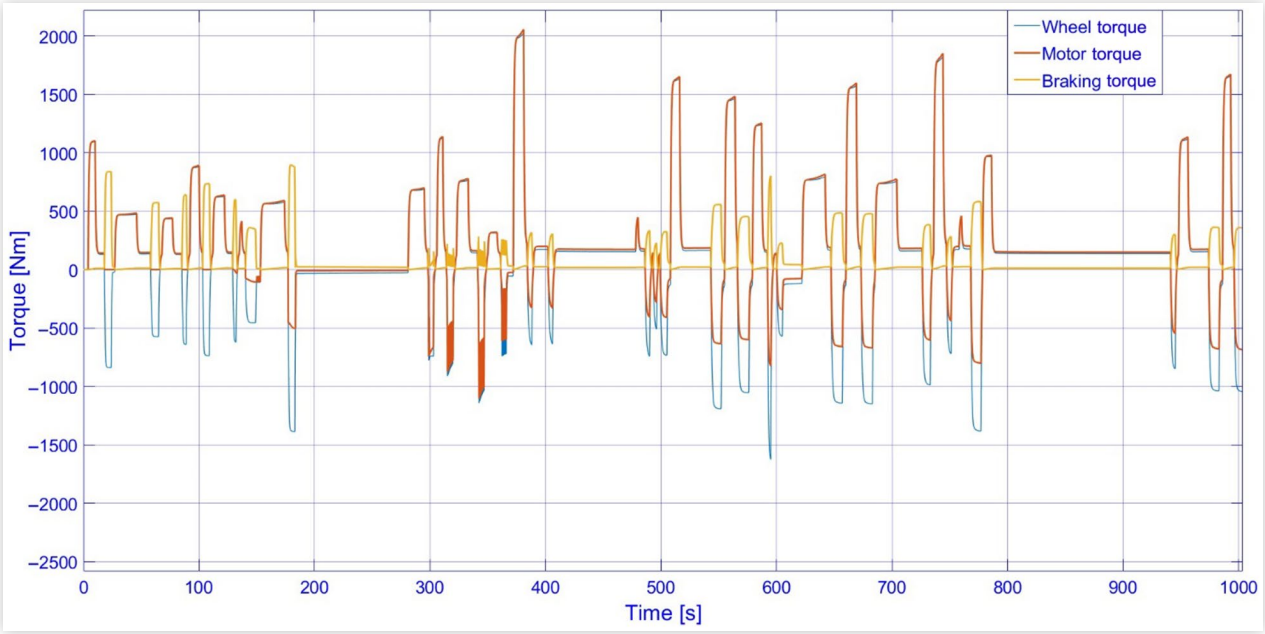

FIGURE 17 Total torque for four motors and for four brakes—Test 6.

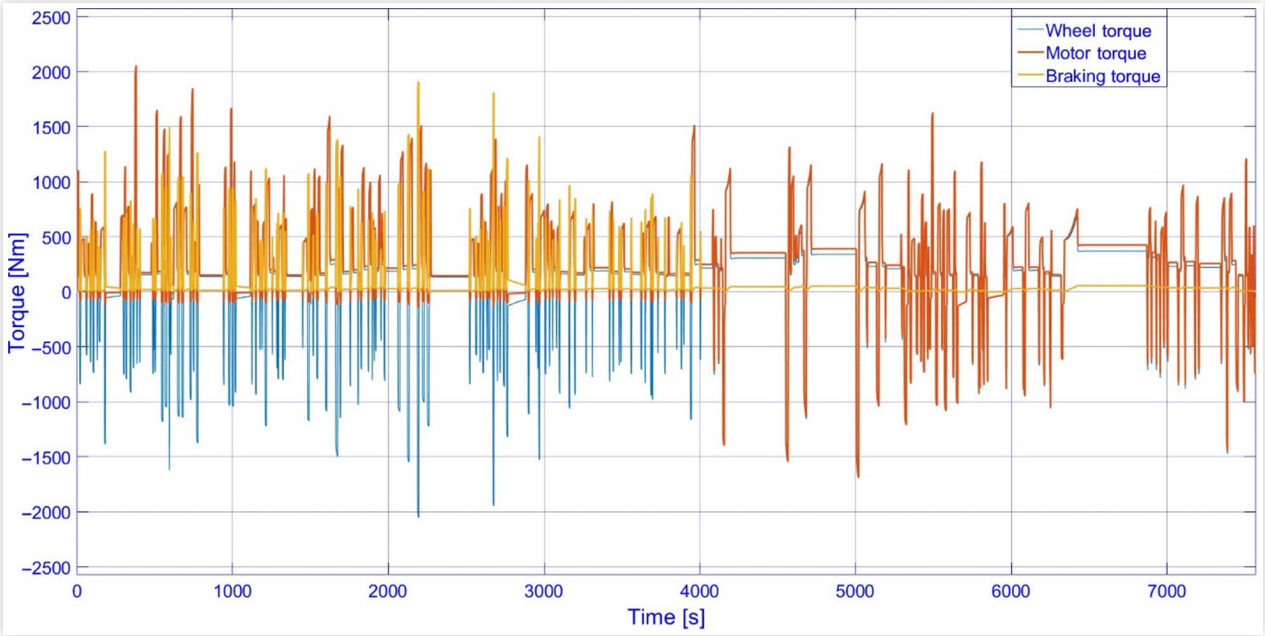

FIGURE 18 Total torque for four motors and four brakes—Test 6 and first 350 s non citata.

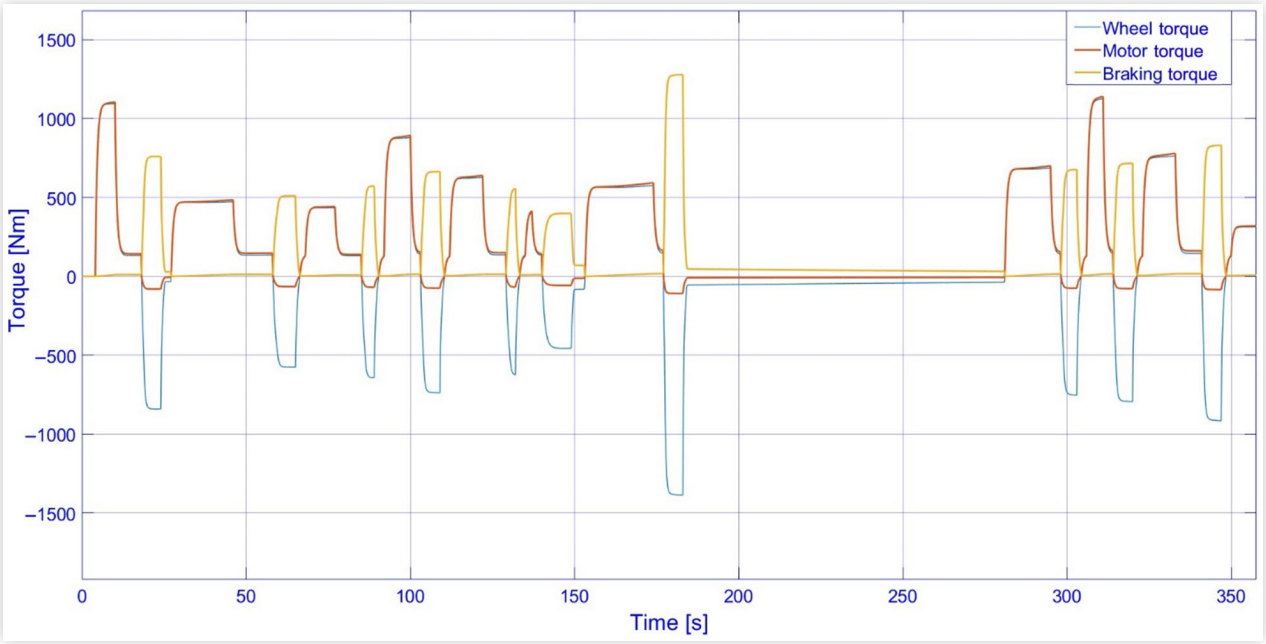

Disconnected configuration in the first 4000 s of simulation (Figure 18), until the SoC drops below 90%. So, during this entire first phase, the energy consumption during braking is zero. The threshold value of 90% was chosen for the following reason: the Disconnected configuration is activated when the battery reaches 98% in the charging phase, so as to prevent regenerative efficiency from being cancelled. Assuming, however, that the vehicle starts at 100% SoC and discharges, if this threshold does not change, when the SoC drops below 98% the logic immediately commands it to return to Baseline configuration. Baseline would result in maximizing RB, and the battery would recharge again, so the logic would find itself commanding the Disconnected configuration again if the SoC reached 98% again. Therefore, for attaining control stability during the battery discharge phase, it was necessary to lower the threshold for disabling Disconnected to 90%. However, this value depends on the battery pack and how its SoC affects regenerative efficiency, so it does not have global significance. It can be modified to achieve better energy optimization.

The control logic imposes the Disconnected configuration in the first 4000 s (Figure 18 shows the first 350 s) of the simulation, until the SoC drops below 90%. So, during this entire first phase, the energy consumption during braking is zero. Figure 19 highlights when the switch from *Disconnected* to *Baseline* is made (after 4100 s). Using these two configurations, particularly *Disconnected* in the first phase, puts slightly more stress on the MR brakes in favor of the electric motors and battery.

The MRF temperature trends obtained in Test 5 and Test 6 are reported in Figure 20, where it is possible to note that during the first phase of *Disconnected* the magnetorheological brakes touch slightly higher temperature peaks than those obtained in Test 5. However, these values are well below the maximum allowable value for an MRF.

Regarding temperatures of the electric motors (Figure 21) again, the *Disconnected* phase has the advantage of stressing the engine much less under braking and maintaining a lower average temperature than that obtained in Test 5; in fact, the maximum value in Test 6 does not exceed 80°C.

It should be specified, however, that the implemented EM thermal model does not consider any cooling system, so the resulting temperature values are certainly overestimated. This choice, which is certainly more conservative, however, does not compromise the validity of the results since the goal is to demonstrate the energy and functional optimization achieved by the braking control logic. So, the realization of a more realistic thermal model for electric motors will certainly be a future priority, which will certainly be facilitated by the outcomes that will be obtained from the ZEDS test bench tests (Figure 22).

It can be concluded that the use of braking control logic in Test 6 results is an energy savings of about 710 Wh compared to the total consumption obtained in Test 5 (Table 5).

FIGURE 19 Total torque for four motors and four brakes—Test 6.

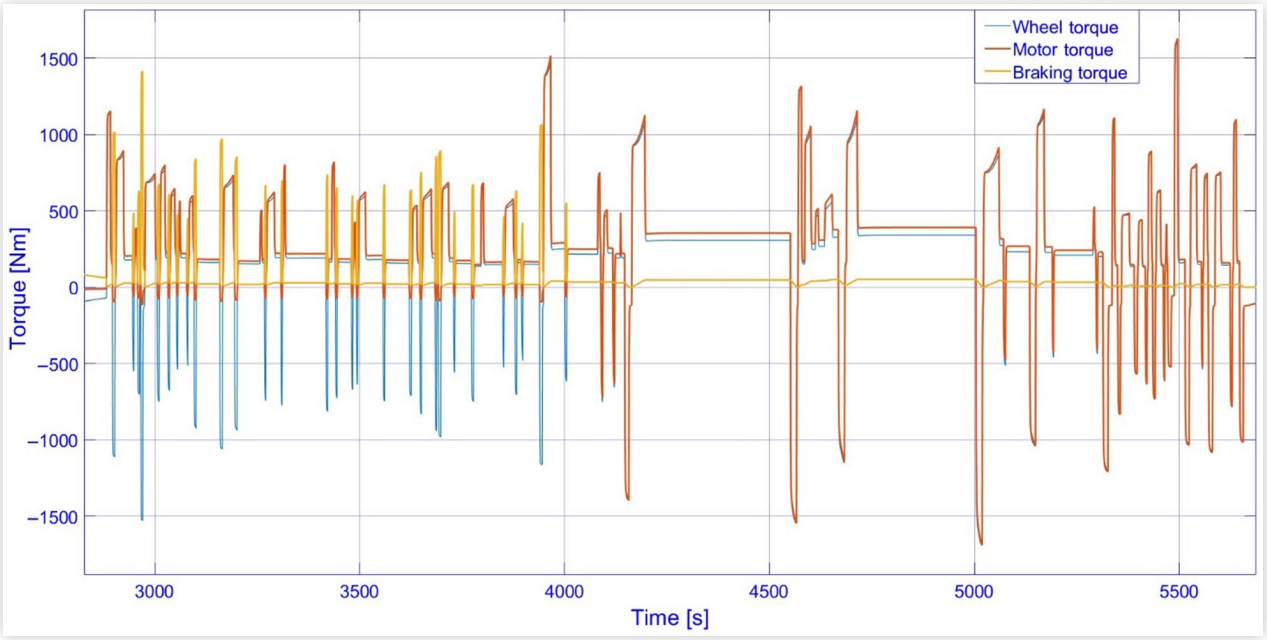

FIGURE 20 MRF temperature [K] in the left front brake—Test 5 and Test 6.

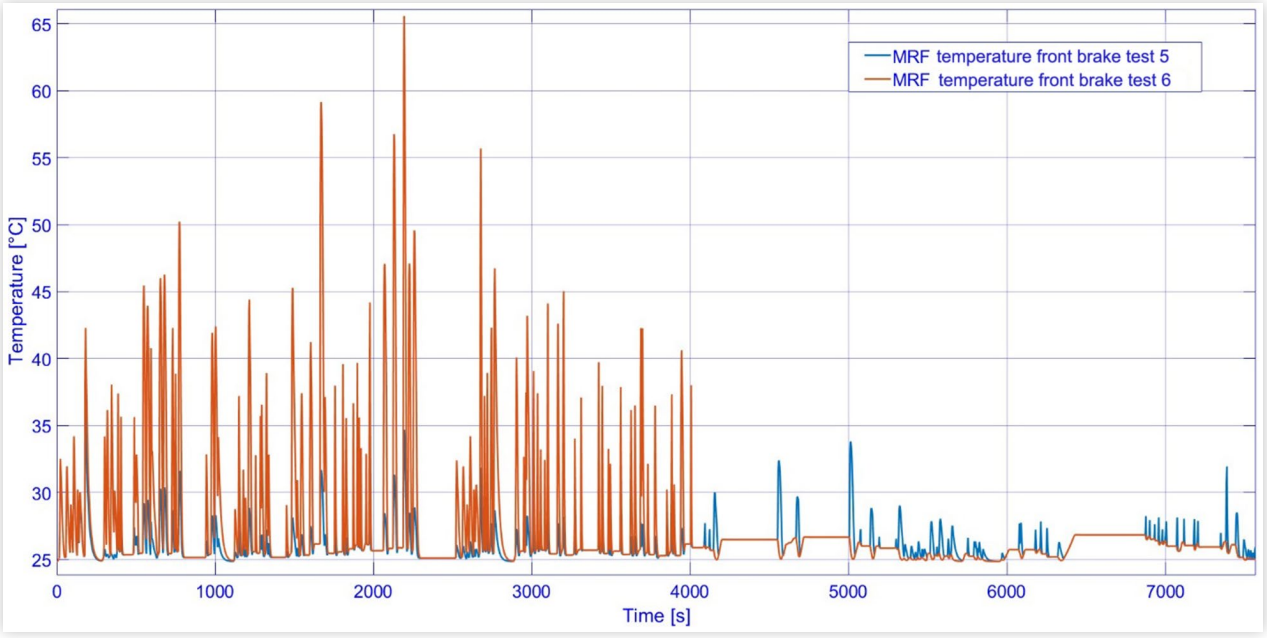

FIGURE 21 Temperature of the left front EM—Test 5 and Test 6.

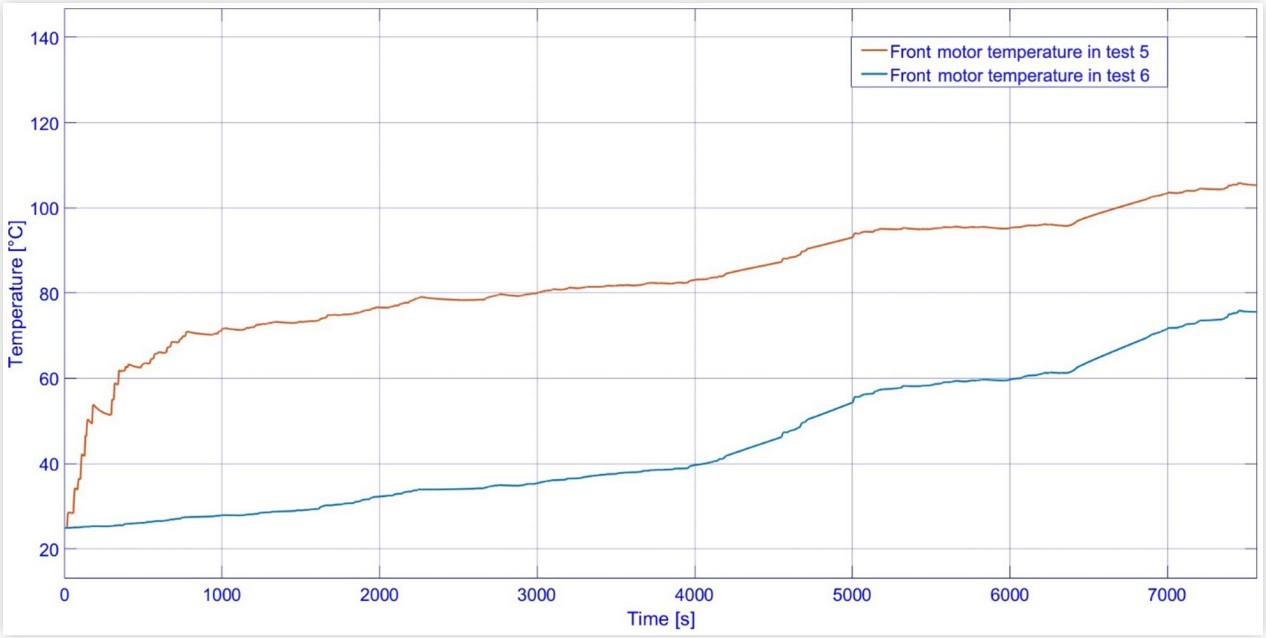

FIGURE 22 SoC—Test 5 and Test 6.

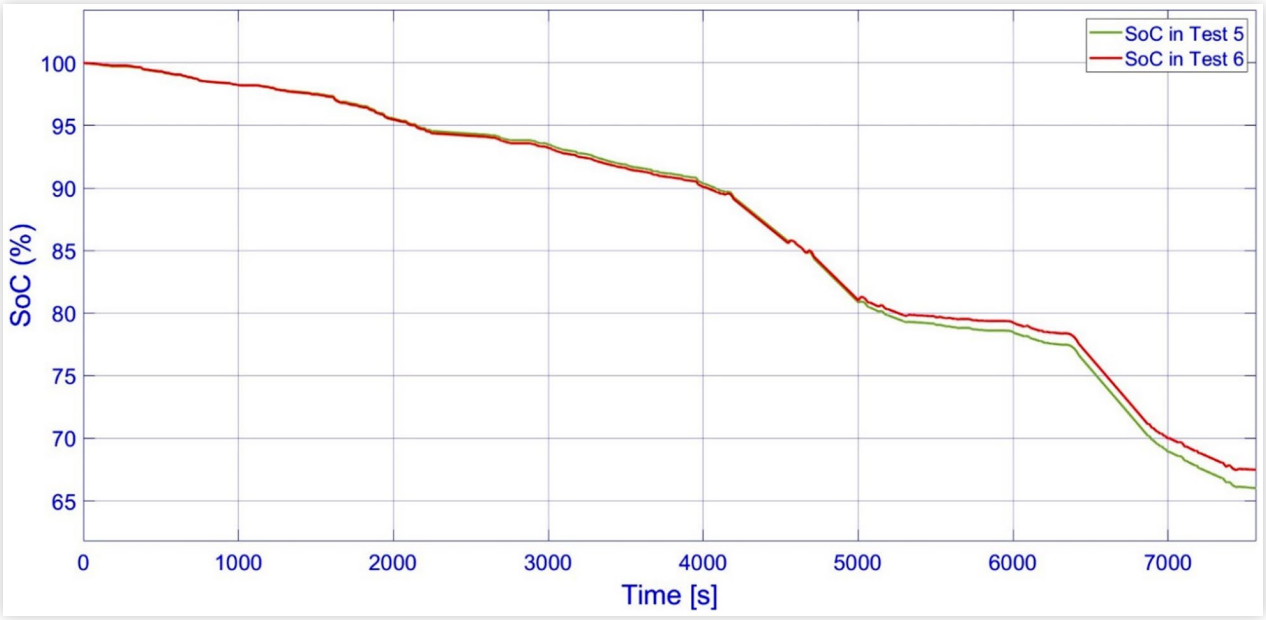

TABLE 5 Results of Test 5 and Test 6.

	Test 5	Test 6	% Difference
Final SoC (%)	66.02	67.49	2.23
Maximum MRF temperature [K]	315.8	341.6	8.17
Energy stored [Wh]	$-1.712 \cdot 10^4$	$-1.641 \cdot 10^4$	4.15

5. Conclusions

One of the major advantages of EVs is their ability to recover energy by exploiting RB. However, the close dependence between regenerative efficiency and the SoC of the battery pack presents a major obstacle to optimizing energy consumption.

BBW has enabled the development of a braking control logic that manages the braking split between the electric motor and the electro-actuated brake in a way that optimizes energy consumption and preserves an optimal operating condition of the electric motors, the brakes, and the battery pack.

A Simulink model was developed with which to simulate the application of control logic during a braking maneuver of an electric vehicle with four in-wheel motors and four innovative electro-actuated brakes. Specifically, two tests were conducted, which simulated the vehicle's descent from Grossglockner Mountain: the first test was conducted with a parallel defined braking configuration, and the second test was conducted with the application of the innovative braking control logic. The results obtained showed a significant reduction in energy consumption in Test 2 compared to Test 1 and reduced brake thermal stress in Test 2, compared to that obtained in Test 1. Another important confirmation of the efficiency of the control logic was obtained with Test 3 and Test 4, in which the descent from Grossglockner Mountain was simulated starting with a battery SoC of 100%, in Test 3 with parallel configuration and in Test 4 applying the control logic. Since the control logic allows the use of RB even at high states of charge, Test 4 reported an optimized energy consumption of 43.64%. A test termed WLTP Brake Cycle was also performed, through which a much longer-lived maneuver is simulated. Again, the result obtained through the application of control logic was better than that obtained with the parallel configuration, with an improvement in energy consumption of 4.15%.The simulation result allows us to establish that the Simulink model is very useful because it allows the braking control logic to be tested not only for the case study analyzed (electric vehicle with four in-wheel motors and four electro-actuated MR brakes) but also with other types of electric vehicles as long as they are equipped with electro-actuated brakes.

For the future step, a control unit using a HiL test bench will be designed, capable of distributing the braking required by the four torque values (over each of the ZEDS), respecting the braking control logic described in the article. The objective is to create a board with the explained algorithm so that it respects all the necessary protocols inherent to the transfer of signals for a high-level control unit in the automotive sector. In this way, once the card has been validated on a HiL test bench, it will be possible to move on to validation on a real vehicle. In addition, for better validation of the described logic, it is necessary to optimize the MATLAB/Simulink model for the simulation environment. In particular, it is important to introduce the vertical and lateral dynamics of the vehicle and tire modeling of the vehicle into the model [30, 31, 32, 33].

Contact Information

Giuseppe Pio Tempone, corresponding author
Phone: +39 3893439037
giuseppe.tempone@polito.it

Massimiliana Carello
Phone: +39 3665610939
massimiliana.carello@polito.it

Henrique de Carvalho Pinheiro
Phone: +39 3511139495
henrique.decarvalho@polito.it

Giovanni Imberti
Phone: +39 3276521344
giovanni.imberti@polito.it

References

1. Ferraris, A., Airale, A.G., Messana, A., Xu, S. et al., "The Regenerative Braking for a L7E Range Extender Hybrid Vehicle," in *2018 IEEE International Conference on Environment and Electrical Engineering and 2018 IEEE Industrial and Commercial Power Systems Europe (EEEIC/I&CPS Europe)*, Palermo, Italy, 2018, 1-7, doi:https://doi.org/10.1109/EEEIC.2018.8494000.
2. European Commission, "Euro 7," November 10, 2022.
3. Li, L., Zhang, Y., Yang, C., Yan, B. et al., "Model Predictive Control-Based Efficient Energy Recovery Control Strategy for Regenerative Braking System of Hybrid Electric Bus," *Energy Conversion and Management* 111 (2016): 299-314, doi:https://doi.org/10.1016/j.enconman.2015.12.077.
4. Tavernini, D. et al., "An Explicit Nonlinear Model Predictive ABS Controller for Electro-Hydraulic Braking Systems," *IEEE Trans. Ind. Electron.* 67, no. 5 (2020): 3990-4001, doi:https://doi.org/10.1109/TIE.2019.2916387.
5. Peng, H. and Chen, X., "Active Safety Control of X-by-Wire Electric Vehicles: A Survey," *SAE Int. J. Veh. Dyn., Stab., and NVH* 6, no. 2 (2022): 115-133, doi:https://doi.org/10.4271/10-06-02-0008.
6. Wagner, D., Steinsträter, M., Förth, M., Stohwasser, M. et al., "Battery Independent Regenerative Braking Using Model Predictive Control with Auxiliary Power Consumers," *Forsch Ingenieurwes* 83 (2019): 843-852.

7. Imberti, G., de Carvalho Pinheiro, H., and Carello, M., "Impact of the Braking System Generated Pollutants on the Global Vehicle Emissions: A Review," in *ICESE*, Leuven, Belgium, 2023.
8. Yang, Y., He, Q., Chen, Y., and Fu, C., "Efficiency Optimization and Control Strategy of Regenerative Braking System with Dual Motor," *Energies* 13, no. 3 (2020): 711, doi:https://doi.org/10.3390/en13030711.
9. Qiu, C., Wang, G., Meng, M., and Shen, Y., "A Novel Control Strategy of Regenerative Braking System for Electric Vehicles under Safety Critical Driving Situations," *Energy* 149 (2018): 329-340, doi:https://doi.org/10.1016/j.energy.2018.02.046.
10. Wang, F., Yin, X., Luo, H., and Huang, Y., "A Series Regenerative Braking Control Strategy Based on Hybrid-Power," in *2012 International Conference on Computer Distributed Control and Intelligent Environmental Monitoring*, Zhangjiajie, China, 2012, doi:https://doi.org/10.1109/CDCIEM.2012.22.
11. Andrieux, A., Lengellé, R., Beauseroy, P., and Chabanon, C., "A Novel Approach to Real Time Tire-Road Grip and Slip Monitoring," *IFAC Proceedings Volumes* 41, no. 2 (2008): 7104-7109, doi:https://doi.org/10.3182/20080706-5-KR-1001.01204.
12. Singh, K.B. and Taheri, S., "Estimation of Tire–Road Friction Coefficient and Its Application in Chassis Control Systems," *Syst. Sci. Control Eng.* 3 (2014): 39-61, doi:https://doi.org/10.1080/21642583.2014.985804.
13. Gobbi, M., Botero, J.C., and Mastinu, G., "Improving the Active Safety of Road Vehicles by Sensing Forces and Moments at the Wheels," *Vehicle System Dynamics* 46, no. S1 (2008): 957-968, doi:https://doi.org/10.1080/00423110802037198.
14. Suomi, A.J., "Wheel Force Transducers (WFT) Brochure," Michigan Scientific Corporation, accessed March 19, 2024, https://www.michsci.com/download/wheel-force-transducers-wft-brochure/.
15. Tempone, G.P., De Carlo, M., and Carello, M., "1D Control Model of a Hydrogen-Powered Vehicle for Race Strategy Optimization," in *2023 IEEE International Conference on Environment and Electrical Engineering and 2023 IEEE Industrial and Commercial Power Systems Europe (EEEIC/I&CPS Europe)*, Madrid, Spain, 2023, doi:https://doi.org/10.1109/EEEIC/ICPSEurope57605.2023.10194634.
16. De Carlo, M., Tempone, G.P., Dragone, P., and Carello, M., "3DOF Vehicle Dynamics Model for Fuel Consumption Estimation," SAE Technical Paper 2024-01-2757 (2024), doi:https://doi.org/10.4271/2024-01-2757.
17. de Carvalho Pinheiro, H., Imberti, G., and Carello, M., "Pre-Design and Feasibility Analysis of a Magneto-Rheological Braking System for Electric Vehicles," SAE Technical Paper 2023-01-0888 (2023), doi:https://doi.org/10.4271/2023-01-0888.
18. Imberti, G., Pinheiro, H.D.C., and Carello, M., "Design of an Innovative Zero-Emissions Braking System for Vehicles," in *2022 International Conference on Electrical, Computer, Communications and Mechatronics Engineering (ICECCME)*, Maldives, 2022.
19. Wang, J. and Li, J., "Hierarchical Coordinated Control Method of In-Wheel Motor Drive Electric Vehicle Based on Energy Optimization," *World Electric Vehicle Journal* 10, no. 2 (2019): 15, doi:https://doi.org/10.3390/wevj10020015.
20. De Novellis, L., Sorniotti, A., Gruber, P., and Pennycott, A., "Comparison of Feedback Control Techniques for Torque-Vectoring Control of Fully Electric Vehicles," *IEEE Transactions on Vehicular Technology* 63, no. 8 (2014): 3612-3623, doi:https://doi.org/10.1109/TVT.2014.2305475.
21. de Carvalho Pinheiro, H., Galanzino, E., Messana, A., Sisca, L. et al., "All-Wheel Drive Electric Vehicle Modeling and Performance Optimization," SAE Technical Paper 2019-36-0197 (2020), doi:https://doi.org/10.4271/2019-36-0197.
22. de Carvalho Pinheiro, H. et al., "Dynamic Performance Comparison between In-Wheel and On-Board Motor Battery Electric Vehicles," in *ASME 2020 International Design Engineering Technical Conferences and Computers and Information in Engineering Conference*, Virtual, Online, November 2020, American Society of Mechanical Engineers Digital Collection, doi:https://doi.org/10.1115/DETC2020-22306.
23. Vignati, M., Sabbioni, E., and Tarsitano, D., "Torque Vectoring Control for IWM Vehicles," *Int. J. Veh. Perform.* 2, no. 3 (2016): 302, doi:https://doi.org/10.1504/IJVP.2016.078561.
24. Bianco, E., Rizzello, A., Ferraris, A., and Carello, M., "Modeling and Experimental Validation of Vehicle's Electric Powertrain," in *2022 IEEE International Conference on Environment and Electrical Engineering and 2022 IEEE Industrial and Commercial Power Systems Europe (EEEIC/I&CPS Europe)*, Prague, Czech Republic, 2022, doi:https://doi.org/10.1109/EEEIC/ICPSEurope54979.2022.9854612.
25. Tempone, G.P., Imberti, G., de Carvalho Pinheiro, H., and Carello, M., "Innovative Zero-Emissions Braking System: Performance Analysis through a Transient Braking Model," SAE Technical Paper 2024-01-2553 (2024), doi:https://doi.org/10.4271/2024-01-2553.
26. de Carvalho Pinheiro, H., "PerfECT Design Tool: Electric Vehicle Modelling and Experimental Validation," *World Electric Vehicle Journal* 14, no. 12 (2023): 337, doi:https://doi.org/10.3390/wevj14120337.
27. EMRAX Innovative, "Manual for EMRAX Motors," 2020.
28. Stewart, W., Fernando, S., and Sims, R., "FEA Simulations for Comparison to Thermal Data Obtained from Vehicle Testing on the Grossglockner High Alpine Road," EURAC Poole Ltd, 2016.
29. Maia, R., Silva, M., Araújo, R., and Nunes, U., "Electrical Vehicle Modeling: A Fuzzy Logic Model for Regenerative Braking," *Expert Systems with Applications* 42, no. 22 (2015): 8504-8519.
30. Savant, S., De Carvalho Pinheiro, H., Sacchi, M.E., Conti, C. et al., "Tires and Vehicle Lateral Dynamic Performance: A Corrective Algorithm for the Influence of Temperature,"

Machines 11, no. 6 (2023): 654, doi:https://doi.org/10.3390/machines11060654.

31. Farroni, F., Sakhnevych, A., and Timpone, F., "Physical Modelling of Tire Wear for the Analysis of the Influence of Thermal and Frictional Effects on Vehicle Performance," *Proceedings of the Institution of Mechanical Engineers, Part L: Journal of Materials: Design and Applications* 231, no. 1-2 (2017): 151-161, doi:https://doi.org/10.1177/1464420716666610.
32. Pacejka, H.B., "Chapter 1: Tire Characteristics and Vehicle Handling and Stability," in: Elsevier Ltd, *Tire and Vehicle Dynamics*, 3rd ed. (2012), https://www.google.it/books/edition/Tire_and_Vehicle_Dynamics/ETnzam6qS2oC?hl=pt-BR&gbpv=1&dq=Tyre+and+Vehicle+Dynamics+3rd+edition&printsec=frontcover.
33. Farroni, F., "TRICK-Tire/Road Interaction Characterization & Knowledge—A Tool for the Evaluation of Tire and Vehicle Performances in Outdoor Test Sessions," *Mechanical Systems and Signal Processing* 72 (2016): 808-831, doi:https://doi.org/10.1016/j.ymssp.2015.11.019.